Toward a Density-Based Representation of Reactivity: S_N2 Reaction

Erika H. Knoerr* and M. E. Eberhart

Department of Chemistry and Geochemistry, 1500 Illinois St., Colorado School of Mines, Golden, Colorado 80401

Received: August 8, 2000; In Final Form: November 3, 2000

The application of quantum mechanics to the study of chemical reactivity has traditionally proceeded with the first-principles calculations of energy-based parameters. Comparison of the energies of the reactant, product, and transition state successfully reveals reactivity trends within similar reactions. However, conceptually, reactions are visualized in terms of the ease with which charge density can be redistributed from reactants to products. With the ready availability of quantum mechanical tools to the chemist, it is necessary that the conceptual and computational pictures of chemical reactivity be unified. Here we show a correlation between energy-based parameters determined from first-principles calculations and features of the charge redistribution accompanying a series of S_N2 reactions. We believe this study will serve as a first step in a more complete, density-based theory of chemical reactivity. Combined with first-principles techniques, this theory will provide the synthetic chemist with a more robust capability to control chemical reactivity.

1. Introduction

Among the important scientific accomplishments of the last century is the development of the quantum theory of matter. Using this theory, the electronic origins for many of the properties of molecular systems have been clarified and rigorous quantum mechanically based theories of molecular and solid-state behavior are emerging.

Concurrent with the development and use of quantum theory has come a less rigorous, but tremendously powerful, semiempirical model of molecular and solid-state properties. Much of this model is based on the work of such investigators as Lewis[1] and Pauling[2] who successfully sought a rationale from which to synthesize organic molecules. Unfortunately, this model makes use of concepts for which it is difficult or impossible to provide rigorous quantum mechanical definitions. For example, the concept of Pauling electronegativity, which figures prominently in the semiempirical model as a basis for explaining the relative reactivity of similar molecules, is a purely empirical parameter that has not been defined quantum mechanically. Consequently, it has proved difficult to make the ever-increasing power of quantum chemistry useful to the synthetic chemists who, by and large, employ the concepts of the semiempirical model.

The semiempirical model is density based, providing a foundation from which to predict the nature of the charge redistribution associated with a given chemical process. In turn, knowledge of this charge redistribution is often all that is necessary to account for the extent of a reaction and the relative stability of its reactants and products. Alternatively, most quantum mechanical models of reactivity are energy based, though there are exceptions.[3,4] However, as the methods of quantum mechanics allow one to calculate a density as well as an energy there is no a priori reason that quantum mechanical rigor cannot be brought to the semiempirical model. As a first step toward this end, we use first-principles methods to model a series of S_N2 reactions and seek a canonical set of quantum mechanically determined, density-based parameters, which can be used to correctly predict observed relative reactivities.

A typical approach toward the quantum mechanical study of chemical reactions is to determine the internal energy of reactants as they move along a reaction coordinate. Here the coordinate is the path of minimum internal energy taking the reactants to the products. The saddle point along such a path is called reaction barrier and the configuration at this point is called the transition state, TS.

A familiar method for displaying this information is the potential energy profile, where the molecular configuration along the reaction coordinate and its corresponding energy are plotted on the *x*- and *y*-axis, respectively. In this representation the energy of the reactant, product, and the transition state, as well as the *x* coordinate of the TS are the crucial parameters. Using these parameters for a similar set of reactions, reactivity trends can be deduced. Though this approach is successful in predicting these trends, the TS energies must be known. Another graphical method, utilizing comparative energy values to predict relative reactivity, is the state correlation diagrams (SCDs)[5] (Figure 1a,b). For a nucleophilic reaction, such as an S_N2 reaction, the SCD consists of the potential energy profiles for two half-reactions (Figure 1a,b). The reaction pathways of identity and nonidentity S_N2 equations are represented by the lowest energy state of the combined reaction and correspond to the inverted cup of the bottom half of the diagram (Figure 1a,b).

In their study of S_N2 reactions, Shaik, Schlegel, and Wolfe[5] identified features of the SCD from which relative reactivity could be inferred. They consider three characteristics as indicative of this reactivity: the ability of the reactant to transfer charge to the product, the stability of the product relative to the reactant, and the localization of charge. Each characteristic quantified by a corresponding energy-based parameter. The interactions of these three measures determine relative reactivity.

These energy-based parameters of the SCD are consistent with established reactivity trends, yet how these parameters are related to the charge redistribution accompanying the formation

* Corresponding author. E-mail: eknoerr@mines.edu. Fax: 303-278-9648.

10.1021/jp0028711 CCC: $20.00
Published on Web 01/11/2001

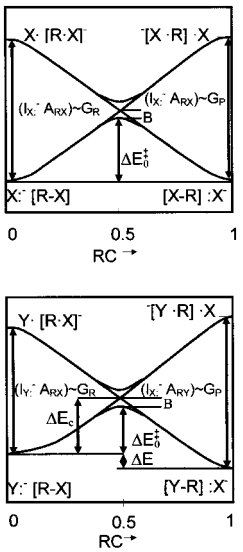

Figure 1. (a, top) and (b, bottom). The state-correlation diagrams of an identity (top), eq 1, and a nonidentity (bottom), eq 2, S_N2 reaction. For a nonidentity S_N2 reaction, (b) $X:^- + [R-X] \rightarrow [X-R-X]^- \rightarrow [X-R] + :X^-$ (eq 1) and $Y:^- + [R-X] \rightarrow [Y-R-X]^- \rightarrow [Y-R] + :X^-$ (eq 2) curves with negative and positive slopes trace the reaction pathways of eqs 3 and 4, respectively, where the curves begin and end at energy values of the reactants and $Y:^- + [R-X] \rightarrow [Y\cdot R] + \cdot X$ (eq 3) and $Y\cdot + [R\cdot X]- \rightarrow [Y-R] + :X^-$ (eq 4) products. The chemical species at the anchors of the diagram, the ground states of the reactant and product, and the vertical charge transfer states of the reactant and product are labeled at the four corners. The thermodynamic driving force, ΔE, the intrinsic barrier, $\Delta E_0^{\ddagger}$, the energy of the crossing point, ΔE_c, the avoided crossing gap, B, and the electron-transfer energy gaps, $(I_{Y:}{}^{-}A_{RX})$ or G_R and $(I_{X:}{}^{-}A_{RY})$ or G_P are labeled, respectively.

of products remains unclear. We believe that first-principles calculations will be more useful to those who now employ the semiempirical model if the energy based parameters can be tied to a density-based "cause". In this paper, we report on correlations between features of the quantum mechanically determined charge density and the energy-based measures of Shaik, Schlegel, and Wolfe describing the charge transfer, stability, and charge localization accompanying an S_N2 reaction.

2. Background

2.1. Reactivity Trends of SN2 Reactions. Shaik, Schlegel, and Wolfe[5] pictured S_N2 reactions in terms of parameters of the state correlation diagram (SCD). The S_N2 reaction is described by the interaction and crossing of two curves, which represent two substitution reactions leading to different charge transfer states (Figure 1). The vertical axis measures the energy difference between charge transfer states, e.g., $Y^- + R-X$ and $Y + [R-X]^-$, while the horizontal axis is the reaction coordinate, giving the configuration as X substitutes for Y in both possible charge transfer states. This gives rise to two possible reaction profiles; the one observed is the one of lowest energy. The gap between the two charge transfer states and denoted G_R or $(I_{Y:}{}^{-}A_{RX})$ in Figure 1 is the electron transfer energy gap. This is the amount of energy it takes to transfer an electron from the nucleophile, $:Y^-$, to the leaving group. The gap designated G_P or $(I_{X:}{}^{-}A_{RY})$ in Figure 1 is the amount of energy required to transfer an electron from $:X^-$ to the forming group. The curves have an avoided crossing gap, B, which describes the difference between the energy at which the curves cross and the transition state. The energy of the crossing point, ΔE_c, is the difference of the energy of the crossing point and the reactant. The intrinsic barrier, $\Delta E_0^{\ddagger}$, is the difference of the energy of the transition state and the reactant. The thermodynamic barrier, ΔE, is the difference in the energies of the product and the reactant.

Shaik et al.[5] have argued that reactivity is a consequence of two parameters: the intrinsic barrier, $\Delta E_0^{\ddagger}$, and the thermodynamic driving force, ΔE. If the intrinsic barriers are identical within a series of reactions, then an increase in ΔE causes a decrease in reactivity. Similarly, if the thermodynamic forces are alike, an increase in the intrinsic barriers causes a decrease in reactivity. The intrinsic barriers are affected by the slopes of the curves and the electron-transfer energy gaps, G_R and G_P. Conceptually, G_R is observed to be related to the ease with which charge is redistributed between the two charge transfer states. If it takes a large amount of energy to move the charge, G_R will be large. The slopes of the curves are related to the localization of charge. If there is a higher degree of charge delocalization within the states, $[CH_3\cdot X]^-$ or $[CH_3\cdot Y]^-$ and $Y\cdot$ or $X\cdot$, the two odd electrons will not pair until the stabilizing effect of the charge delocalization is overcome. This requires the reactants to be comparatively close and forces arched curves and a higher intrinsic barrier. In summary, Shaik et al. determine that a reaction with high reactivity entails very little energy to move charge, has a much more thermodynamically stable product than reactant and localized charge transfer states.

2.2. Electron Density. Our approach to constructing density-based analogues of the energy-based parameters of Shaik et al. is to begin with Bader's theory of atoms in molecules (AIM).[6] Bader has shown that an atom existing as a distinguishable unit within a molecule can be justified equivalently on topological and quantum mechanical grounds. Here we make use of the topological definitions of atoms and bond paths. This topology of a molecule is determined by that of its corresponding charge density. In turn, this topology is determined by the character of the density in the neighborhood of a finite number of points where the gradient of the charge density vanishes, i.e., critical points (CPs). The character of a critical point, CP, is denoted by an index of two numbers; the first number is simply the number of dimensions of space and the second number is the net number of positive curvatures. For example, a minimum CP has positive curvature in all three orthogonal directions; therefore, it is called a (3, 3) CP. A maximum would be denoted by (3, −3), since all three curvatures are negative. A saddle point with two of the three curvatures negative is denoted (3, −1), while the other saddle point is a (3, 1) CP.

Bader[6] realized that the classification of molecular electron density in terms of the positions of its critical points could be used to describe chemical structure and bonding. For example, bonds in molecules can be associated with specific topological features of the electron density. A bond path is seen as the ridge of maximum electron density connecting two nuclei. The existence of such a ridge is guaranteed by the presence of a (3, −1) CP between the bound nuclei. The charge density along such a path must be a maximum with respect to any neighboring path. Because a (3, −1) CP is both a necessary and sufficient condition for the existence of a bond path, this critical point is referred to as a bond critical point, BCP. Other types of critical points have been correlated with additional features of molecular structure. A (3, 1) CP is required at the center of ring structures like benzene. Accordingly, this critical point has been designated as a ring critical point. A minimum within a cage structure, characterized by a single (3, 3) CP, has been given the descriptive name of a cage critical point.

TABLE 1: Total Charge Density, the Curvatures, the Laplacian, the Gaussian Curvature, the Measure of the Extent of Bond Formation, and Localization at the C−X Bond Critical Point Listed for Each Molecule (Values in electrons/bohr^3)

	CH_3F	CH_3Cl	CH_3Br	CH_4	CH_3CN
λ_0	0.2354	0.1766	0.1287	0.2774	0.2651
λ_1	0.4300	0.2728	0.1641	0.7312	0.5088
λ_2	0.4300	0.2727	0.1641	0.7312	0.5088
λ_3	0.7176	0.314	0.2289	0.4971	0.3208
$l_1 + \lambda_2 + \lambda_3$	0.1424	0.2315	0.09936	0.9652	0.6968
$\lambda_1\lambda_2\lambda_3$	0.1327	0.02336	6.164E2	0.2658	0.08305
$\lambda_0 \sin^2 \theta$	0.1472	0.09452	0.07496	0.1122	0.1025
x	0.3555	0.3067	0.2389	0.7698	0.4880

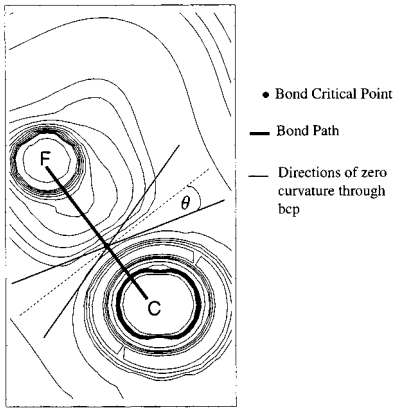

Figure 2. A contour plot of the charge density at the bcp between the carbon and fluorine within the methyl fluoride molecule. The line between the carbon and fluorine traces the bond path. The line at angle θ from the line perpendicular to the bond path is the direction of zero curvature. When the charge density moves the line of zero curvature to the line perpendicular to the bond path, $\theta = 0$, the bond will break.

3. Electron Density Based Measures

In an S_N2 reaction, the bond between carbon and the leaving group is well formed at the beginning of the reaction. Charge must be moved from this bond and into the forming bond between the carbon and the nucleophile as the reaction proceeds. To first order this charge redistribution may be followed by analyzing the changes in density at the breaking and developing BCPs. The nature of the charge density in a neighborhood of a CP may be described to second order by four parameters: λ_0, λ_1, λ_2, and λ_3. Where λ_0 is the total electron density, λ_1 and λ_2 are the extreme curvatures perpendicular to the bond path in two orthogonal directions and λ_3 is the curvature parallel to the bond path. For the specific examples given in this paper $\lambda_1 = \lambda_2$.

To examine the curvatures at the BCP, molecular structures for the reactants and products of select S_N2 reactions were optimized and checked by frequency calculations employing Gaussian 98[7,8,9] with B3LYP/6-311+G(3DF,3PD)//B3LYP/6-31+G(D) calculations. The values of the curvatures for the BCP of the breaking and forming bonds in select S_N2 reactions were evaluated in an AIM[6] calculation during the single point computation. These curvatures are listed in Table 1.

3.1. Charge Transfer. To quantify the charge redistribution at a bond critical point we have defined a parameter, which varies continuously from zero to some positive value as a bond is formed. As an example, consider the electron density in any plane containing the carbon−fluoride bond of methyl fluoride, Figure 2. At the BCP and lying in this plane, there is a pair of directions in which the curvature is zero. As a bond is stretched during a chemical reaction the angle θ shown in Figure 2 will change, forcing the directions of zero curvature to swing away from the bond path. When this angle vanishes, the direction of zero curvature becomes perpendicular to the bond path and by definition the bond has broken.[10−13] Therefore, the quantity $\lambda_0 \sin^2 \theta$ is a parameter that varies continuously with the formation of a bond. We call the quantity $\lambda_0 \sin^2 \theta$ the "extent of bond formation". Now using the same rationale as that employed in transition state theory, we can argue that this same quantity is related to the amount of charge that must be lost from a BCP in

$$\lambda_0 \sin^2 \theta = \lambda_0 \frac{\lambda_1}{\lambda_1 + \lambda_3} \tag{1}$$

order to break its bond. Since the extent of bond formation is a measure of the amount of charge required for bond breaking/forming, it should correlate with charge transfer. Thus, we postulate that the total amount of charge minus the amount of charge needed to break the bond, eq 2, should be the total amount of charge, which needs to be

$$\Delta q \propto (\lambda_0^{\,p} + \lambda_0^{\,r}) - (\lambda_0^{\,p} \sin^2 \theta_{\text{product}} + \lambda_0^{\,r} \sin^2 \theta_{\text{reactant}})$$

$$\Delta q \propto \lambda_0^{\,p} \cos^2 \theta_{\text{product}} + \lambda_0^{\,r} \cos^2 \theta_{\text{reactant}} \tag{2}$$

moved throughout the reaction.

The correlation of Δq with charge transfer is shown in Table 2. As expected, Δq correlates well with the intrinsic barrier. For example, the amount of charge required to move in an S_N2 reaction, where fluorine is the leaving group and hydrogen is the forming group, is greater than the amount of charge necessary to move in an S_N2 reaction where bromine is the leaving group and hydrogen is the forming group. Consequently, the reaction requiring the greater movement of charge has the lower reactivity and the higher intrinsic barrier.

3.2. Stability and Localization. We investigated several features of the charge density which had the potential to correlate with stability. Initially, we compared the Laplacian of the charge density at a BCP to the energetic parameter of Shaik et al. that was argued to measure stability. This approach was motivated by Bader who has reasoned that if the charge is concentrated at the BCP, the forces on the nuclei are attractive and the virial of the nuclear forces stabilizes the system. If the charge is depleted at the BCP, the forces on the nuclei are repulsive and the virial of the nuclear forces destabilize the system. The measure of the concentration/depletion of charge Bader uses is the Laplacian, which is the sum of the principal curvatures, λ_1, λ_2, and λ_3. He proposed that if the Laplacian is negative or positive, the charge is concentrated or depleted, respectively. Therefore, Bader predicts that a molecule possessing concentrated charge at the BCPs is more stable than a molecule possessing depleted charge at the BCPs. Alternativly, Zheng and Boyd discovered that the total charge within the BCP of the leaving group in the TS correlated with the thermodynamic driving force of the reaction, ΔE.[14] We considered various measures that would correspond to the stabilization of the charge, i.e., the Laplacian and the Gaussian curvature (the product of the principal curvatures) (Table 1). These measures were compared with the computed total energy values.[5,7−9] We found that the best measure of stability is $\Delta\lambda_0$, calculated by the total charge at the BCP of the product minus that of the reactant (eq 3). We interpret this difference to indicate how stable

$$\Delta\lambda_0 \propto \lambda_{0\text{product}} - \lambda_{0\text{reactant}} \tag{3}$$

TABLE 2: Correlation of $\Delta E_0^{\ddagger}$, ΔE, and Position of TS with Δq, $\Delta\lambda_0$, and Ratio of Localization, Respectively[a]

reaction series	$\Delta E_0^{\ddagger}(4)$ (kcal/mol)	Δq[b] (electrons/bohr^3)	$\Delta E(4)$ (kcal/mol)	$\Delta\lambda_0$ (electrons/ bohr^3)	position of TS $x^{\ddagger}(4)$[c]	ratio of localizn $\xi_{react}/(\xi_{react}+\xi_{prod})$
H,H	52	0.3302	0	0	0.5	0.5
CN,CN	28.5	0.3251	0	0	0.5	0.5
F,F	20	0.1764	0	0	0.5	0.5
Cl,Cl	15.7	0.1642	0	0	0.5	0.5
Br,Br	11.6	0.1075	0	0	0.5	0.5
F,Cl	18.2	0.1703	28	0.0587	0.437	0.463
Cl,Cl	10.2	0.1642	0	0	0.5	0.5
Br,Cl	N/A	0.1359	8	0.0479	0.516	0.562
CN,F	28.2	0.2508	5	0.0297	0.463	0.421
CN,Cl	9.4	0.2447	32	0.0884	0.411	0.386
CN,Br	7.4	0.2163	40	0.1364	0.387	0.329
H,F	15.4	0.2533	57	0.0420	0.212	0.318
H,Cl	2.7	0.2472	86	0.1007	0.177	0.287
H,Br	N/A	0.2188	94	0.1487	0.167	0.239

[a] The reactions are defined as Y, X, in the reaction $CH_3X + Y^- \rightarrow CH_3Y + X^-$. [b] The value of Δq in the identity equations will increase or decrease slightly depending on the values of ξ, the localization factor. For example, the reaction H,H will have a slightly higher Δq, because its ξ value is high. [c] The position of the TS using energy terms was calculated with eq 6.30.[1]

the forming bond within the product is relative to the breaking bond in the reactant. For example, in Table 2, for a forward reaction such as F,Cl, $\Delta\lambda_0$ is positive, there is more total charge density at the bcp between C and F than C and Cl, and thus the C−F bcp is more stable than the C−Cl. For a reverse reaction such as Br,Cl, $\Delta\lambda_0$ is negative, there is more total charge at the bcp between C and Cl than C and Br, and thus the C−Cl BCP is more stable than the C−Br BCP. Therefore, if the charge is greater at the BCP of the product relative to the reactant indicating a large $\Delta\lambda_0$ for a reaction, the reactivity will tend to be high. The correlation of $\Delta\lambda_0$ with stability can be seen in Table 2, which lists the measure of the amount of charge transfer required for each reaction to occur relative to the thermodynamic driving force for the reaction.

Finally, a correlation between features of the charge density and charge localization was found, where charge concentration is pictured in terms of electron density per distance. This representation of localization is identified to be ξ, where D is the C−X bond length

$$\xi = \lambda_0 \frac{D}{d} \tag{4}$$

and d is the distance from X to the BCP. When the distance from X to the BCP is small and the bond length is large, the charge is concentrated in the leaving group, forcing the D/d ratio to be large, thus ξ to be large. Additionally, the more charge that can be held in the BCP of the leaving group (large λ_0), the larger the localization term, ξ, and therefore the more concentrated the charge. If the charge at the BCP of the product is more localized than the reactant, the TS has a tendency to occur early. In Table 1 the BCP of C−Cl is more localized than C−Br, but less localized than C−F, thus in the F,Cl and Br,Cl reactions the TS would tend to be early and late, respectively.

As discussed above, the relative amount of localization of charge within the C−X bond of the reactants and products is determined by the value of ξ. The position of the TS on the x-axis is determined by the localization properties of the reactant relative to the product;[1] therefore, we sought a correlation between the ratio of localization of the reactant as in eq 5 and the position of the TS on the x-axis, Table 2. We found such a correlation

$$\Xi = \frac{\xi_{\text{react}}}{\xi_{\text{react}} + \xi_{\text{prod}}} \tag{5}$$

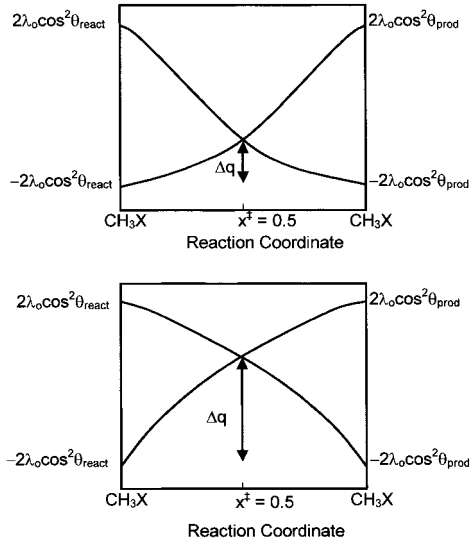

Figure 3. Examples of identity reactions where the localization terms, ξ, are small and large, top and bottom, respectively.

where we define Ξ to be the degree of localization of the reactant relative to the product.

Applying these measures, diagrams analogous to the SCDs can be constructed for identity S_N2 reactions. Similar to the SCDs, the x-axis is the reaction coordinate, but the y-axis is now a measure of electron density. The identity reactions have one curve with a negative slope beginning at $x = 0$ and $y = 2\lambda_0 \cos^2\theta$ of the reactant, crossing the positively sloped curve at $x = 0.5$, and ending at $x = 1$ with the value of $y = -2\lambda_0 \cos^2\theta$ of the product (Figure 3). The other curve has a positive slope beginning with $y = -2\lambda_0 \cos^2\theta$ of the reactant, crossing the negatively sloped curve at $x = 0.5$, and ending with the value of $2\lambda_0 \cos^2\theta$ of the product. The curvatures of the identity reactions can be analyzed by means of the value of ξ, where a large value of ξ predicts that the curves are the most arched or the least bowed of all the reactions and small value of ξ predicts the curves are the least arched or the most bowed. These comparable electron density based diagrams are consistent with the observed SCDs.

Diagrams analogous to the SCDs can be constructed for nonidentity S_N2 reactions as well. The nonidentity reactions have a positively sloped curve beginning with the $(-\lambda_0 + -2\lambda_0 \cos^2\theta)$ value of the reactant (Figure 4a,c). It passes through the TS at a y value determined by Δq and ends with a value on the

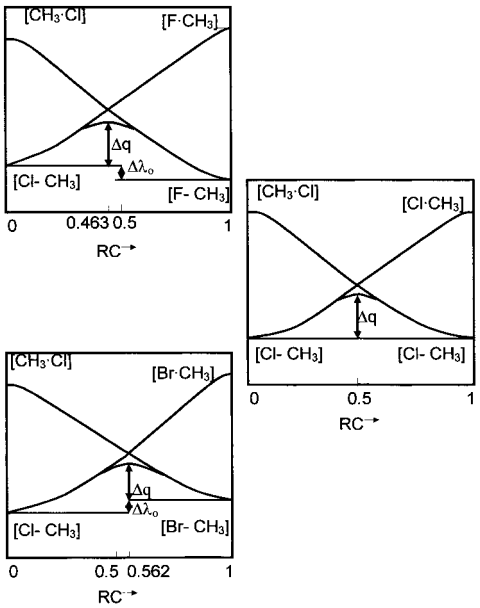

Figure 4. (a, top), (b, middle), and (c, bottom): All three diagrams are modified SCDs. The top diagram is an example of a nonidentity reaction such as F,Cl where the transition state occurs early. The middle diagram is an example of an identity reaction such as Cl,Cl where the transition state occurs at 0.5. The bottom diagram is an example of a nonidentity reaction such as Br,Cl where the transition state occurs late.

y-axis dictated by Ξ. The negatively sloped curve begins with a value on the *y*-axis that is influenced by Ξ, passes through the TS at the *y* value controlled by Δq, and ends with the $(-\lambda_0 + 2\lambda_0 \cos^2 \theta)$ value of the product. Using the localization values, we can predict where the TS will occur on the *x*-axis; and therefore, approximate the *y*-axis points of the curves. If the product is more localized than the reactant (Figure 4a), the negatively sloped curve bows and the positively sloped curve arches, forcing the TS position on the *x*-axis to be early. If the reactant is more localized than the product (Figure 4c), the positively sloped curve bows and the negatively sloped curve arches, directing the TS position on the *x*-axis to be late. Accordingly, for the series of X,Cl reactions in Figure 4, a, b, and c, the TS of the F,Cl reaction within that series occurs early, therefore the diagram of F,Cl (Figure 4a) has a negatively sloped curve that is the most arched and a positively sloped curve that is the most bowed within the series. The TS for the Br,Cl reaction occurs late, and therefore the diagram of Br,Cl (Figure 4c) has a positively sloped curve that is the most bowed and a negatively sloped curve that is the most arched within the series. Thinking about the position of the TS on the reaction coordinate in terms of the movement of electron density, these trends are supported. If an electron within the bond between the carbon and the leaving group in the reactant is delocalized, the electron can move easily from the bond. This electron must overcome the larger electron−electron repulsion in the more localized bond but once localized in the forming bond it is tightly held. The comparable electron density based diagrams for nonidentity reactions are consistent with the observed SCD diagrams and significantly; no information about the electron density at the TS is required.

In conclusion, knowledge and analysis of the electron density of the reactants and products alone provides a novel method to predict reactivity. Charge transfer and thermodynamic driving forces of a reaction are described using density-based terms such as Δq and $\Delta\lambda_0$. The localization term, ξ, relates to the degree of concentration of the charge in the BCP of the breaking and forming bonds. The ratio of the localization term, Ξ, predicted the relative position of the TS on the reaction coordinate. These terms correlate well with their energy-based counterparts, predicting the reactivity of several simple model S_N2 reactions. In summary, these terms come from the distinct difference in the depiction of charge at the BCP of the leaving and forming bonds between reactions with an early versus late TS. In a reaction with an early TS, the breaking bond has a BCP with a smaller amount of delocalized charge that spreads perpendicular to the bond path and a forming BCP is characterized by a larger amount of localized charge that is more narrowly spread along the bond path.

Acknowledgment. The authors thank the Air Force Office of Scientific Research and the donors of the Petroleum Research Fund, administered by the ACS, for support of this research.

References and Notes

(1) Lewis, G. N. *J. Am. Chem. Soc.* **1916**, *38*, 762.
(2) Pauling, L. *The Nature of the Chemical Bond*; Cornell University Press: Ithaca, NY, 1960.
(3) Bader, R. F. W.; MacDougal, P. J. *J. Am. Chem. Soc.* **1985**, *107*, 6788−6795.
(4) Bader, R. F. W.; Duke, A. J.; Messer, R. R. *J. Am. Chem. Soc.* **1973**, *95*, 7715−7721.
(5) Shaik, S. S.; Schlegel, H. B.; Wolfe, S. *Theoretical Aspects of Physical Organic Chemistry: The S_N2 Mechanism*; John Wiley & Sons: New York, 1992.
(6) Bader, R. F. W. *Atoms in Molecules: A Quantum Theory*; Clarendon Press: Oxford, UK, 1995.
(7) Frisch, A.; Frisch, M. J. *Gaussian 98 User's Reference*; Gaussian Inc.: Pittsburgh, PA, 1994−1999.
(8) Foresman, J. B.; Frisch, A. *Exploring Chemistry with Electronic Structure Methods*; Gaussian Inc.: Pittsburgh, PA, 1996.
(9) Frisch, M. J.; Trucks, G. W.; Schlegel, H. B.; Scuseria, G. E.; Robb, M. A.; Cheeseman, J. R.; Zakrzewski, V. G.; Montgomery, J. A.; Stratmann, R. E.; Burant, J. C.; Dapprich, S.; Millam, J. M.; Daniels, A. D.; Kudin, K. N.; Strain, M. C.; Farkas, O.; Tomasi, J.; Barone, V.; Cossi, M.; Cammi, R.; Mennucci, B.; Pomelli, C.; Adamo, C.; Clifford, S.; Ochterski, J.; Petersson, G. A.; Ayala, P. Y.; Cui, Q.; Morokuma, K.; Malick, D. K.; Rabuck, A. D.; Raghavachari, K.; Foresman, J. B.; Cioslowski, J.; Ortiz, J. V.; Stefanov, B. B.; Liu, G.; Liashenko, A.; Piskorz, P.; Komaromi, I.; Gomperts, R.; Martin, R. L.; Fox, D. J.; Keith, T.; Al-Laham, M. A.; Peng, C. Y.; Nanayakkara, A.; Gonzalez, C.; Challacombe, M. P.; Gill, M. W.; Johnson, B. G.; Chen, W.; Wong, M. W.; Andres, J. L.; Head-Gordon, M.; Replogle, E. S.; Pople, J. A. *Gaussian 98* (Revision A.7); Gaussian, Inc.: Pittsburgh, PA, 1998.
(10) Eberhart, M. E. *Can. J. Chem.* **1996**, *74*, 1229−1235.
(11) Eberhart, M. E.; Giamei, A. F. *Mater. Sci. Eng. A* **1998**, *248*, 287−295.
(12) Eberhart, M. E. *Acta Metallurg.* **1996**, *44* (6), 2495−2504.
(13) Eberhart, M. E. *Philos. Mag. A* **1996**, *73* (1), 47−60.
(14) Zheng, S.; Boyd, R. J. *J. Am. Chem. Soc.* **1989**, *111*, 1575−1579.